



2-2012

Ablation Test-Case Series #3. Numerical Simulation of Ablative-Material Response: Code and Model Comparisons

Tom van Eekelen
Samtech, Belgium

Jean R. Lachaud
University of California, Santa Cruz

Alexandre Martin
University of Kentucky, alexandre.martin@uky.edu

Ioana Cozmuta
NASA Ames Research Center

Right click to open a feedback form in a new tab to let us know how this document benefits you.

Follow this and additional works at: https://uknowledge.uky.edu/me_facpub

 Part of the [Aerospace Engineering Commons](#)

Repository Citation

van Eekelen, Tom; Lachaud, Jean R.; Martin, Alexandre; and Cozmuta, Ioana, "Ablation Test-Case Series #3. Numerical Simulation of Ablative-Material Response: Code and Model Comparisons" (2012). *Mechanical Engineering Faculty Publications*. 20.
https://uknowledge.uky.edu/me_facpub/20

This Conference Proceeding is brought to you for free and open access by the Mechanical Engineering at UKnowledge. It has been accepted for inclusion in Mechanical Engineering Faculty Publications by an authorized administrator of UKnowledge. For more information, please contact UKnowledge@lsv.uky.edu.

Ablation Test-Case Series #3. Numerical Simulation of Ablative-Material Response: Code and Model Comparisons

Notes/Citation Information

Published in the *Proceedings of the 5th Ablation Workshop*, AW05–053, p. 1-12.

The copyright holder has granted the permission for posting the article here.

ABLATION TEST-CASE SERIES #3
NUMERICAL SIMULATION OF ABLATIVE-MATERIAL RESPONSE: CODE AND MODEL COMPARISONS
VERSION 1.0, FEBRUARY 16, 2012

Tom van Eekelen

LMS - SAMTECH
 Liège, Belgium

Tom.vanEekelen@lmsintl.com

Jean R. Lachaud

UARC, UC Santa Cruz
 NASA Ames, Moffett Field, CA

Jean.R.Lachaud@nasa.gov

Alexandre Martin

Department of Mechanical Engineering
 University of Kentucky, Lexington, KY
 Alexandre.Martin@uky.edu

Ioana Cozmuta

Advanced Supercomputing Division
 STC/NASA Ames, Moffett Field, CA
 Ioana.Cozmuta@nasa.gov

1. INTRODUCTION

The test-case series #3 will be a further extension of the tests defined within the framework of the NASA ablation modelling workshops.^{1,2} In order to reduce the amount of work, all tests within test-case series #3, will use the TACOT material defined by Lachaud et al.² The main goal of this new series, is to test the 3D modelling capabilities of the participating codes. The first 1D results were presented at the 4th Ablation workshop,³ and together with the results of the second test-case series, will be discussed and analyzed more thoroughly at the 5th Ablation Workshop, Feb. 28- March 1, 2012, Lexington, Kentucky.

1.1. Summary of the first test-case

The first test case was defined for the 4th Ablation Workshop, 1-3 March 2011, Albuquerque, New Mexico.¹ It was a one-dimensional test case focusing on the in-depth material response - fixed surface temperature and no recession. Three types of material-response codes have been identified:

- Type 1: based on the CMA⁴ model or any mathematically equivalent model (heat transfer, pyrolysis, simplified mass transport);
- Type 2: CMA-type + Averaged momentum equation for the transport of the pyrolysis gases;
- Type 3: Higher fidelity codes (chemical/thermal non-equilibrium, etc).

The results had been provided by the participants before the workshop and a summary was presented during the workshop.³ For type 1 and type 2 codes, differences in the temperature prediction were mostly below 1%.

1.2. Summary of the second test-case series

The definition of the test case series #2 was finalized in Lachaud et al.,² and the results of all the participants will be compared at the 5th Ablation Workshop. A traditional B' table was provided to facilitate the in-depth material-response comparison but other tables/methods could be used. A specific test-case dedicated to the estimation of the ablation rate was also proposed. A total of four tests were defined:

- 2.1: low heating, no recession (targeted surface temperature of about 1644 K, cf. test-case 1) - non-physical intermediate case without recession in preparation for 2.2.
- 2.2: low heating (same as test case 2.1), recession

- 2.3: high heating, recession (targeted surface temperature of about 3000 K)
- 2.4: computation of the ablation rate of the material of the second test case for a temperature range of 300K-4000K and an air pressure of 101325 Pa (1 atm.). The B'-table format was used to enable visual comparison.

2. DESCRIPTION OF THE THIRD TEST-CASE SERIES

In series #3 two test cases are foreseen, the first test-case is mandatory while the second one will be discussed by the participants. Both tests will be presented at the 5th Ablation Workshop, Feb. 28- March 1, 2012, and the tests will be performed by all the participants in the ablation modeling working group (dates discussed during 5th Ablation Workshop).

- The mandatory test: This test consists of an "iso-q" calorimeter^{5,6} made of TACOT subjected to an enthalpy form heat flux. A total of three tests are performed where every tests has an increasing level of complexity, namely:
 - An axis-symmetric/3D model with an isotropic version of TACOT.
 - The same model but with an orthotropic version of TACOT.
 - A full 3D model with a non-axis-symmetric heat load.
- The optional tests: The SPRITE model,⁷ using the TACOT material which is subjected to a re-entry trajectory heat load.

3. THE MANDATORY "ISO-Q" TEST-CASE

3.1. Geometry of the test specimen

The geometry of the mandatory test-case is given in Figure 1, where the diameter D equals 10.16 cm. The "iso-q" test-case is chosen because it was shown^{5,6,8} that the ablation will be almost uniform along the surface. As a consequence the shape of the test-specimen will not change during the analysis, and the flow and thermal-structure analysis are decoupled, i.e. the heat load will not change during ablation.

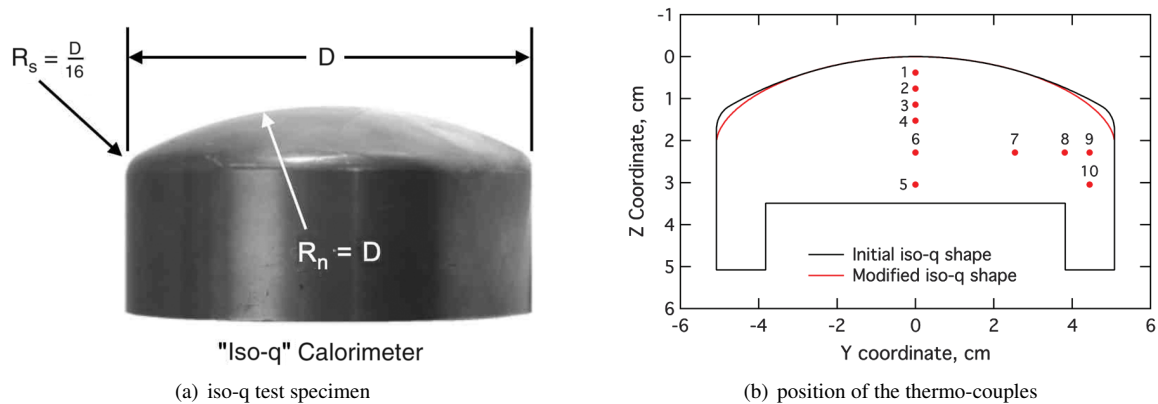


Figure 1: Definition of the geometry and dimensions of the iso-q test specimen.^{5,6,8}

In Figure 1(b) and Table 1 we see the position of the thermo-couples, for which the temperature evolutions have to be post-processed. The thermo-couples are positioned symmetrically with respect to the axis of axis-symmetry (Z-axis). Because both the geometry and the heat load are axis-symmetric, resulting in axis-symmetric results.

The outer geometry of the specimen is completely defined by the additional assumption that the tangents of the two circles (s, n) (see Figure 1(a)) and the circle (s) and the vertical line, at their intersection points are identical. With these assumptions the dimensions given in Figure 2(a) are obtained, and the following coordinate data can be derived:

- position of the $circle_n - circle_s$ intersection point ($y = 4.679$ cm, $z = 1.174$ cm),

Table 1: Coordinates of the thermo-couples.

TC	Y-coordinate [cm]	Z-coordinate [cm]	TC	Y-coordinate [cm]	Z-coordinate [cm]
1	0.00	0.381	6	0.00	2.286
2	0.00	0.762	7	2.540	2.286
3	0.00	1.143	8	3.810	2.286
4	0.00	1.524	9	4.445	2.286
5	0.00	3.048	10	4.445	3.048

- position of center of rotation of $circle_s$ ($y = 4.445$ cm, $z = 1.736$ cm),
- position of the $circle_s$ - vertical line intersection ($y = 5.080$ cm, $z = 1.736$ cm).

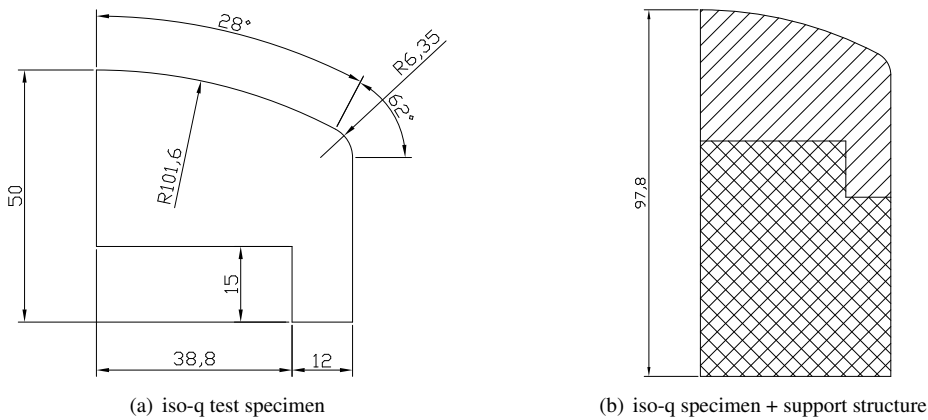


Figure 2: The dimensions [mm] of the iso-q specimen + support structure.

Besides the "iso-q" specimen, a support structure is defined in Figure 2(b). Although the support structure will in general be made of a different material, here we will also assume it is also made of TACOT, and that the contact between the "iso-q" specimen and the support structure is perfect. It is therefore allowed to create one continuous mesh/discretization for the "iso-q" and the support structure. With this geometrical data, the participants will be able to construct their numerical (mesh/grid) models.

3.2. Loads and boundary conditions

The test-specimen is subjected to a similar heat load as applied in test 2.3 of test-case series #2. The specimen will be subjected to a convective heating during the first 40 seconds, and it will cool-down for 1 minute under the hypothesis of radiative cooling only. The initial conditions are: $p_0 = 1$ atm (101325 Pa), $T_0 = 300$ K. The initial gas composition in

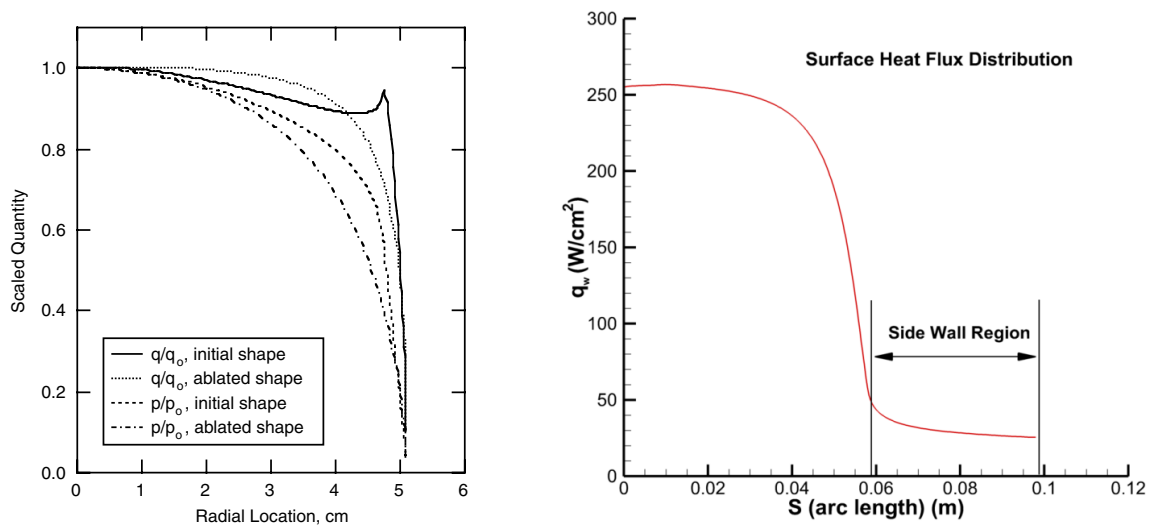
Table 2: Summary of the environment properties. Please use linear interpolation during the 0.1s heating and cooling periods (linear ramping).

time (s)	$\rho_e u_e C_H(0)$ ($\text{kg} \cdot \text{m}^{-2} \cdot \text{s}^{-1}$)	h_e ($\text{J} \cdot \text{kg}^{-1}$)	p_w (Pa)
0	0	0	101325
0.1	0.3	$2.5 \cdot 10^7$	101325
40	0.3	$2.5 \cdot 10^7$	101325
40.1	0	0	101325
120	0	0	101325

the material is left open. For type 1 and 2 codes, pyrolysis gas in thermal equilibrium is the usual practice. For type 3 codes, it is suggested to start with air. The time-dependent boundary-layer properties are summarized in table 2. The other boundary-layer assumptions/properties are as follows for the code comparison:

- The factor for the blowing-correction correlation used is the CMA model is taken as $\lambda = 0.5$.
- Heat and mass transfer assumptions in the boundary layer: $Pr = Le = 1$
- Re-radiation is active during the entire analysis [$q_r = \epsilon\sigma(T_w^4 - T_\infty^4)$]. Due to the convex shape of the test-specimens, a view factor of 1 is used. The infinity temperature is chosen to be $T_\infty = 300$ K .
- Use the wall enthalpy (h_w) and the B'_c table provided in the TACOT_2.2.xls file for code comparison.

The above definition of the heat flux ($q(T_w, t)$) is only 1D and applies to the stagnation point only. In order to extend it to the axis-symmetric geometry of Figure 2(b) we will use the heat flux distribution around the "iso-q" calorimeter + support structure, calculated by Dec et.al.⁹ and Milos and Chen.⁵ In Figure 3(a) the variation of the heat flux and pressure along the



(a) Heating and pressure distributions⁵ for initial and slightly ablated shapes

(b) heating distribution for the iso-q specimen⁹

Figure 3: Heating and pressure distributions^{5,9} for the iso-q specimen.

Table 3: Distribution of the $q_w/q_w(0)$ values as a function of the Y- and Z-coordinate (derived from Figure 3(b)).

s (cm)	Y-coord. (cm)	Z-coord. (cm)	$q_w/q_w(0)$	s (cm)	Y-coord. (cm)	Z-coord. (cm)	$q_w/q_w(0)$
0.00	0.000	0.000	1.000	5.50	5.068	1.617	0.476
2.00	1.987	0.196	1.000	5.75	5.080	1.864	0.261
3.00	2.957	0.439	0.971	6.00	5.080	2.114	0.169
3.50	3.431	0.597	0.955	6.50	5.080	2.614	0.137
4.00	3.898	0.777	0.925	8.00	5.080	4.114	0.111
4.50	4.354	0.980	0.863	10.00	5.080	6.114	0.101
5.00	4.800	1.209	0.743	13.70	5.080	9.780	0.101

test-specimen is given as a fraction of stagnation point load ($q_0, p_0 = p_w$), for the initial and ablated shape. The ablated shape is shown in Figure 1(b), which only has a small local deformation superimposed on an otherwise uniform surface recession.⁵ In order to have a uniform recession during the analysis we have to use the q/q_0 values of the ablated shape. Here we will

use the $q_w(s)$ distribution given by Dec et al.⁹ in Figure 3(b), because it is given in more detail. The pressure is held constant both in time and along the outer surface. The pressure distribution calculated in Milos and Chen⁵ is valid for an impermeable "iso-q" calorimeter, while TACOT will allow for some equalization of the pressure, which will not be modelled in the series #3 test-cases.

For this test-case we will thus apply the heat-flux and pressure profile defined in Figure 3(b), where we premultiply $\rho_e \mu_e C_H(0)$ with the $q_w/q_w(0)$ values in Table 3. We will use the TACOT wall enthalpy h_w and ablation rate B'_c values, obtained for a constant pressure $p_w = p_0$ of 101325 Pa. For the back-side of the support structure we assume an adiabatic, and impermeable for gas, boundary condition.

3.3. Axis-symmetric/3D model

Because the model has an axis-symmetric shape, an axis-symmetric discretization will in principle suffice. Depending on the availability of different numerical models (in the participating codes) the participants may decide to use a 3D segment model instead of an axis-symmetric model. Both the 3D segment model and the axis-symmetric model will give the same results, and can be used for both the isotropic and orthotropic material model.

3.3.1. Model with an isotropic material

The TACOT material definition (TACOT_2.2.xls) is an isotropic definition, and can thus be applied directly to the axis-symmetric/3D model.

3.3.2. Model with an orthotropic material

One of the goals of this test-series, is to compare the modelling capabilities of the different codes. One of the modelling capabilities, of practical interest, is to model orthotropic materials. For example PICA⁵ is known to be orthotropic, where the Through The Thickness conductivity is lower than the isotropic conductivity, and the In Plane conductivity is higher than the isotropic conductivity. We therefore propose to use an orthotropic model, where the conductivities are defined via multiplication factors ($\alpha_1 = 0.9, \alpha_2 = 1.1$) for the isotropic conductivity of the TACOT model.

$$\begin{vmatrix} \lambda_{TT} & 0 \\ 0 & \lambda_{IP} \end{vmatrix} = \begin{vmatrix} \alpha_1 & 0 \\ 0 & \alpha_2 \end{vmatrix} \lambda_{\text{isotropic}} \quad (1)$$

The through the thickness direction is aligned with the axis of axis-symmetry (Z-axis in Figure 1).

3.4. A full 3D model with a 3D heat load definition

A final functionality that will be tested within series #3, is the full 3D modelling capabilities of the participating codes. Because finding a fully 3D physical test is not obvious, we have decided to perform a non-physical test, which is similar in concept to the test shown in Lachaud and Mansour.¹⁰ Here we will use a full 3D "iso-q" model with the orthotropic TACOT material defined in section 3.3.2.

While the pressure distribution will not be modified, the heat-load distribution (from section 3.2) will be modified in such a way that it becomes non-symmetric. The q/q_0 distribution will be multiplied, with a Gaussian distribution, in such a way that a localized heat-flux peak will be added on top of the existing distribution. The multiplication factor will be:

$$f(x,y) = 1 + \beta e^{-\frac{1}{2\sigma^2}[(\mu_x-x)^2+(\mu_y-y)^2]} \quad (2)$$

The Gaussian is determined by the position of its average values ($\mu_x = 0.0$ cm, $\mu_y = 1.0$ cm) and the radius ($2\sigma = 1.0$ cm) in which 95.4 % of the additional power is applied. The nominal heat flux q/q_0 will be increased by a multiplication value of β (= 0.3). This multiplication function will result in a 3D localized heat flux, and thus a 3D solution.

4. THE SMALL RE-ENTRY PROBE TEST-CASE

After testing the participating codes, on all the necessary functionalities for an industrial type application, a re-entry probe model is a logical next step. As an example the SPRITE model, described by Empey et al.,⁷ is used. The definition of the small re-entry probe test case is not yet finalized, and will be the subject of discussions between the workshop participants. The questions that need to be answered are:

- Will we apply a realistic re-entry load, and if so who will be capable and willing to supply this?
- Do we need to model radiative heat exchange (between structure and instruments) inside the capsule?
- How will the geometry of the test-case be defined:
 - will a description, like in Figure 2, be given?
 - will a full 3D CAD model be supplied?
 - will a finite element mesh be supplied?
- what are the results we would like to obtain?
- Which of the participants is able and willing to do this test?

4.1. Geometry of the test specimen

In Figure 4(a) we see a cross section of the SPRITE model given in the paper of Empey et al.⁷ From this paper a 3D model of the probe has been re-created, and it is given in Figure 4(b). The model shown, is available as a CAD file (STEP format) and can be obtained from the authors.

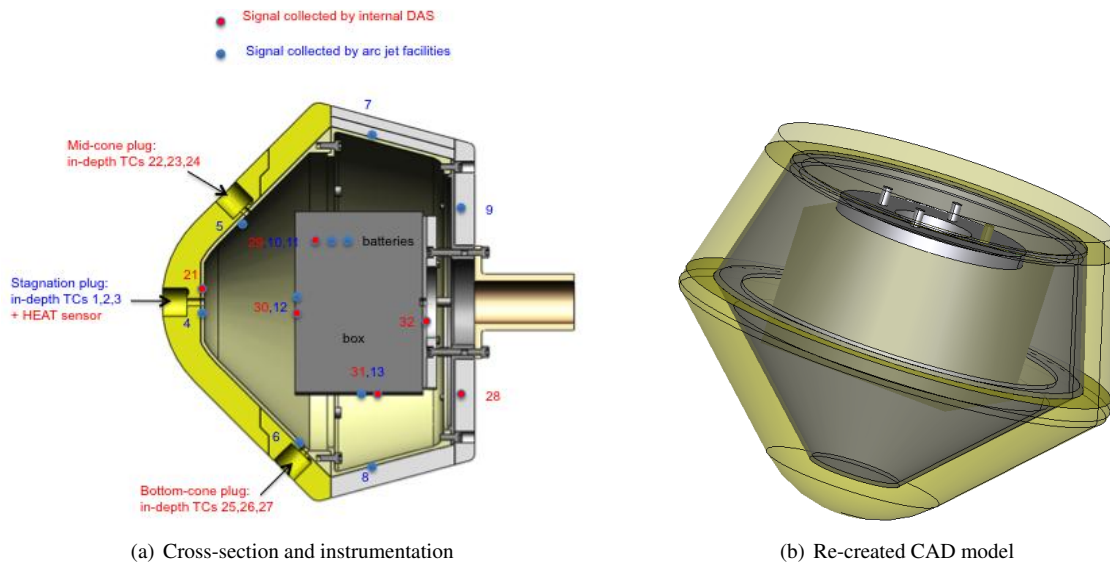


Figure 4: Definition of the SPRITE probe.⁷

4.2. Material definition

For the SPRITE model we will again use the orthotropic version of the TACOT material, as defined in section 3.3.2. In this case the IP direction is perpendicular to the axis of axis-symmetry, i.e. the TTT direction is only perpendicular to the outer surface at the stagnation point.

4.3. Loads and boundary conditions

A uniform initial temperature of 300 K is assumed, after which a re-entry heat flux is applied. This heat flux (convection, radiation) will depend on wall temperature, time and varies with location over the heat shield. The definition of this heat flux will be discussed between the participants.

5. MATERIAL DATA

The material properties for this test-case series are provided and explained in the spreadsheet TACOT_2.2.xls. Recent updates:

- B' table updated (July 28, 2011)
- Equilibrium properties of the pyrolysis gases up to 4000K (June 2011)

6. CODE OUTPUT AND COMPARISON OF THE RESULTS

The code output described in this section will only apply to the results of section 3. The output for the re-entry vehicle will depend on it's definition, which is the subject of ongoing discussions. The results will be supplied in ASCII file format, which contain the following results (with an output frequency of 0.1 s):

- The temperature at the position of the stagnation point and of the 10 thermo-couples will be post-processed. The position of the thermo-couples are defined in Table 1 and Figure 1.
- For the same points (stagnation point and the thermo-couples) also the density will be post-processed.
- The blowing rates, the surface recession and the pyrolysis zone thickness, will be post-processed at the stagnation point. The mass and the position of the centre of gravity, of the "iso-q" specimen, will be calculated. The values to post-process are:
 - Blowing rates: The blowing rates \dot{m}^s and \dot{m}^c are calculated at the outer surface.
 - Pyrolysis zone thickness: The thresholds, to calculate the location of the pyrolysis and char fronts, are defined as: $\rho_v(98\%) = \rho_c + 0.98(\rho_v - \rho_c)$; $\rho_c(2\%) = \rho_c + 0.02(\rho_v - \rho_c)$. The distance is calculated w.r.t. the initial outer surface.
 - Surface recession: The displacement of the point w.r.t. the original position is calculated.
 - Mass: The total mass of the "iso-q" specimen will be calculated as a function of time.
 - Y-coordinate: The y-coordinate of the centre of gravity, of the "iso-q" specimen, as a function of time.

Output format desired:

time (s)	Tw (K)	T1 (K)	T2 (K)	T3 (K)	...	T8 (K)	T9 (K)	T10 (K)
0	3.000e2	3.000e2	3.000e2	3.000e2	3.000e2	3.000e2	3.000e2	3.000e2
0.1	9.651e2	3.225e2	3.000e2	3.000e2	3.000e2	3.000e2	3.000e2	3.000e2
0.2	1.076e3	3.956e2	3.039e2	3.000e2	3.000e2	3.000e2	3.000e2	3.000e2
etc.

Table 4: Output format for the temperature file: CodeName_Energy_TestCase_3-i.txt

time (s)	rhov (kg/m3)	rho1 (kg/m3)	rho2 (kg/m3)	...	rho10 (kg/m3)
0	2.800e2	2.800e2	2.800e2	2.800e2	2.800e2
0.1	2.7900e2	2.800e2	2.800e2	2.800e2	2.800e2
0.2	2.7500e2	2.800e2	2.800e2	2.800e2	2.800e2
etc.

Table 5: Output format for the density file: CodeName_Density_TestCase_3-i.txt

Result files need to be generated for the three test cases of section 3, and the *i* in the file names will refer to:

- *i* = 1: Model with an isotropic material,
- *i* = 2: Model with an orthotropic material,
- *i* = 3: A full 3D model with a 3D heat load definition.

time (s)	m_dot_g (kg/m ² /s)	m_dot_c (kg/m ² /s)	Virgin 98%	Char 2%	recession (m)	Mass (kg)	Y-coord. (m)
0	0	0	0	0	0	1.200E-02	1.200E-02
0.1	5.063e-3	0	0	0	0	1.200E-02	1.200E-02
0.2	1.340e-2	0	1.781e-4	2.130e-5	0	1.200E-02	1.200E-02
etc.

Table 6: Output format for the pyrolysis and ablation-response file: CodeName_Mass_TestCase_3-i.txt

7. PRELIMINARY RESULTS

The results shown are generated with SAMCEF Amaryllis, and serve as a baseline for visual comparison for the test cases. Please do not give them more credit than they deserve and use them for sanity check rather than for comparison.

8. ACKNOWLEDGMENTS

We would like to thank you in advance for any comment that will help to improve the clarity of this document. Please send your comments to the authors.

9. REFERENCES

- [1] Lachaud, J., Martin, A., Cozmuta, I., and Laub, B., “Ablation Workshop Test Case - Version 1.1 - Feb. 2, 2011,” Prepared for the 4th Ablation Workshop (1-3 March 2011. Albuquerque, New Mexico).
- [2] Lachaud, J., Martin, A., van Eekelen, T., and Cozmuta, I., “Ablation test-case series #2 - Version 2.8 - Feb. 6, 2012,” Prepared for the 5th Ablation Workshop (28 February - 1 March 2012. Lexington, Kentucky).
- [3] “Overview of Intercalibration Results,” Thermal Performance Database Team, Oral presentation, 4th Ablation Workshop (1-3 March 2011. Albuquerque, New Mexico).
- [4] Kendall, R. M., Bartlett, E. P., Rindal, R. A., and Moyer, C. B., “An Analysis of the Coupled Chemically Reacting Boundary Layer and Charring Ablator,” Contractor report CR-1060, NASA, 1968.
- [5] Milos, F. and Chen, Y.-K., “Two-Dimensional Ablation, Thermal Response, and Sizing Program for Pyrolyzing Ablators,” *Journal of Spacecraft and Rockets*, Vol. 46, No. 6, December 2009, pp. 1089–1099.
- [6] Agrawal, P., Ellerby, D. T., Switzer, M. R., and Squire, T. H., “Multidimensional Testing of Thermal Protection Materials in the Arcjet Test Facility,” 10th AIAA/ASME Joint Thermophysics and Heat Transfer Conference, No. AIAA 2010-4664, AIAA, 2010.
- [7] Empey, D. M., Skokova, K. A., Agrawal, P., Swanson, G. T., Prabhu, D. K., Peterson, K. H., and Venkatapathy, E., “Small Probe Reentry Investigation for TPS Engineering (SPRITE),” 8th International Planetary Probe Workshop, IPPW-8, Portsmouth, Virginia, 2011.
- [8] Milos, F. and Chen, Y.-K., “Ablation and Thermal Response Property Model Validation for Phenolic Impregnated Carbon Ablator,” *Journal of Spacecraft and Rockets*, Vol. 47, No. 5, September-October 2010, pp. 786–805.
- [9] Dec, J. A., Laub, B., and Braun, R. D., “Two-Dimensional Finite Element Ablative Thermal Response Analysis of an Arcjet Stagnation Test,” 42nd AIAA Thermophysics Conference, No. AIAA 2011-3617, 27-30 June 2011.
- [10] Lachaud, J. and Mansour, N. N., “A pyrolysis and ablation toolbox based on OpenFOAM, with application to material response under high-enthalpy environments,” 5th OpenFOAM Workshop, Chalmers, Gothenburg, Sweden, June 21-24 2010.

Initial results of test-case 3.1

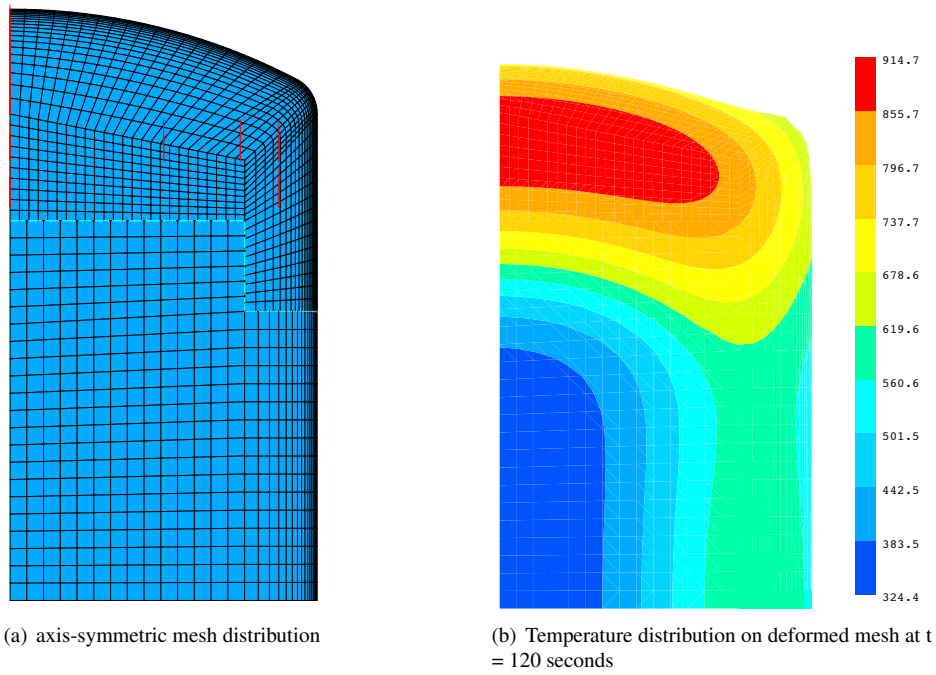


Figure 5: Test3.1: Mesh and temperature distribution of the test-specimen plus the support structure.

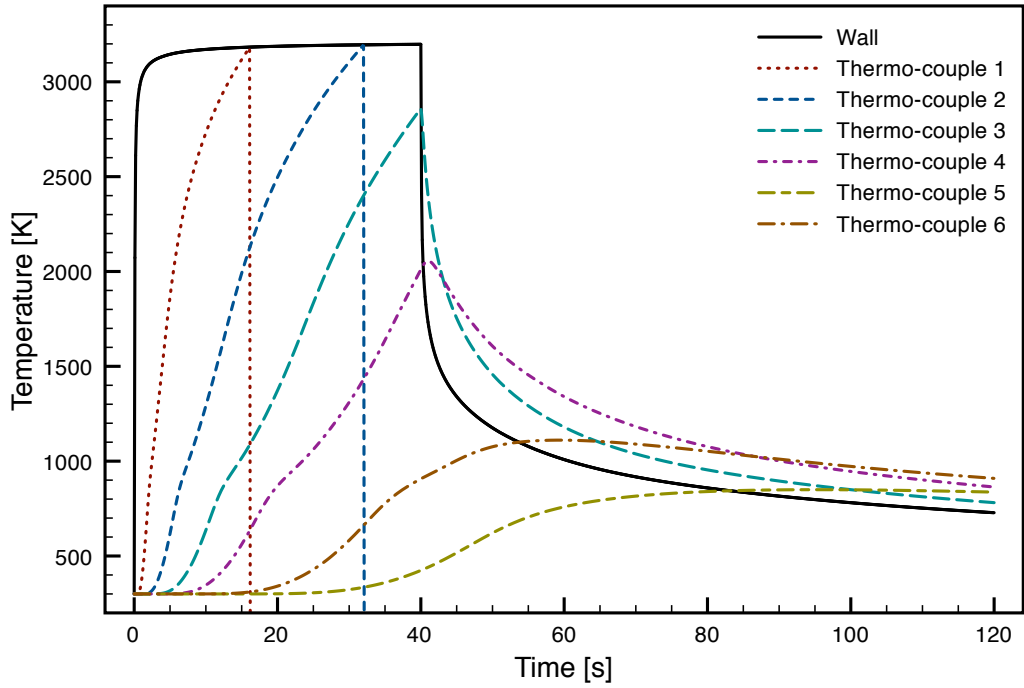


Figure 6: Test3.1: Temperature evolution of the wall and the thermo-couples 1 till 6.

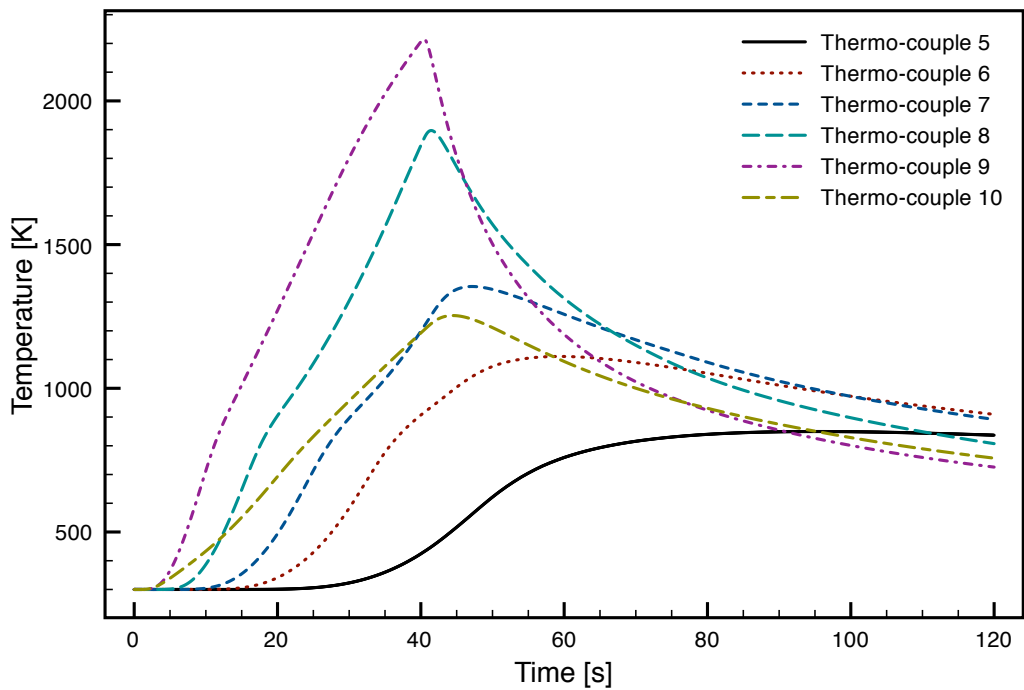


Figure 7: Test3.1: Temperature evolution of the thermo-couples 6 till 10.

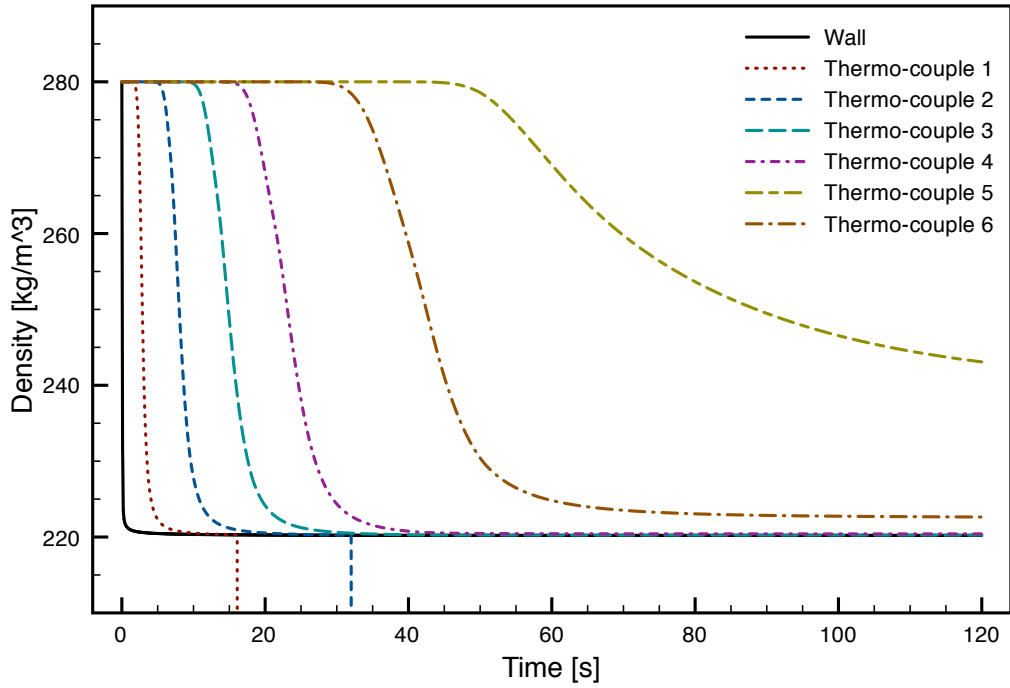


Figure 8: Test3.1: Density evolution of the wall and the thermo-couples 1 till 6.

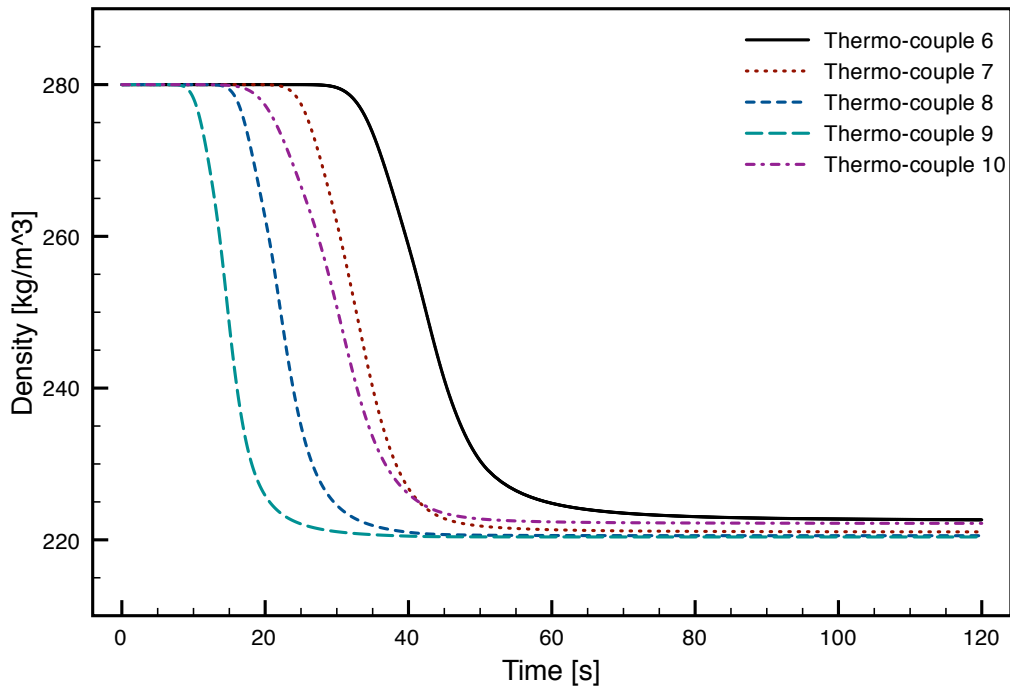


Figure 9: Test3.1: Density evolution of the thermo-couples 6 till 10.

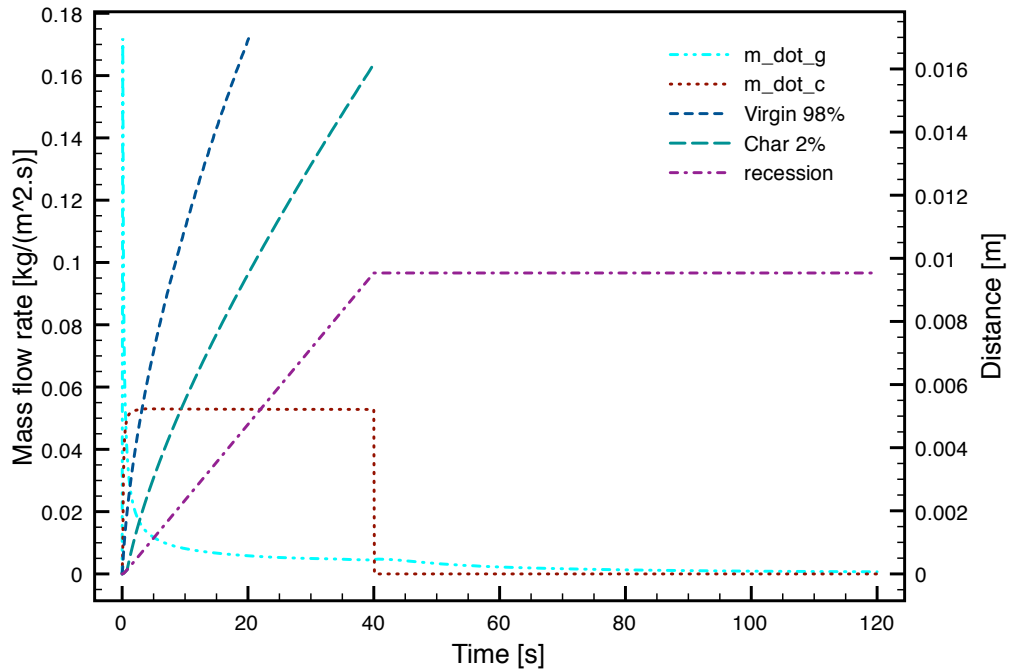


Figure 10: Test3.1: Mass flow rate, wall recession, and (partial) char thickness at the stagnation point.

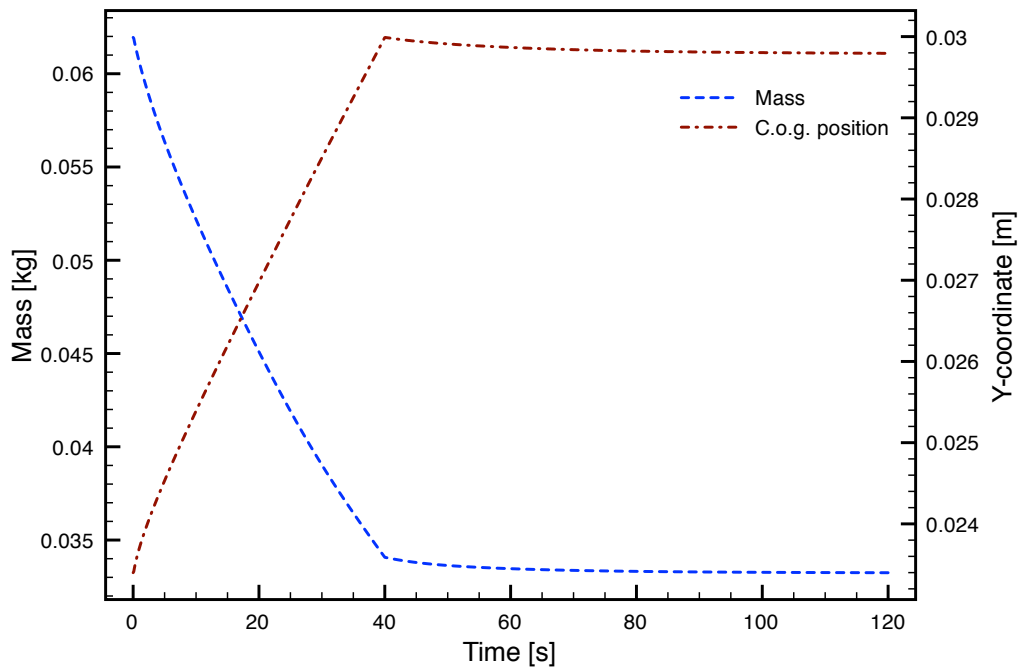


Figure 11: Test3.1: Mass and centre of gravity evolution, of the "iso-q" specimen.